

Creation, manipulation and detection of atomic Josephson vortex

V.M. Kaurov and A.B. Kuklov

*Department of Engineering Science and Physics,
The College of Staten Island, CUNY, Staten Island, New York 10314*

(Dated: February 8, 2020)

We show numerically as well as by employing the variational approach that Josephson vortex (JV), existing in quasi-1D atomic Bose Josephson junction formed by two coupled parallel Bose-Einstein condensate (BEC) waveguides, can be controllably manipulated by imposing a difference of the chemical potentials on the waveguides. This effect has its origin in the Berry phase structure of the vortex. Experimental aspects of creation and detection of the JV with traditional techniques of phase imprinting and absorption imaging are discussed as well. An image of the expanding cloud containing the JV has very distinct features which may allow its unambiguous identification.

PACS numbers: 03.75.Lm, 03.75.Kk, 11.30.Qc

I. INTRODUCTION

From the very beginning of the experimental achievement of Bose-Einstein condensation in trapped ultracold gases, various solitonic and topological collective structures, such as dark [1] and bright [2] solitons, vortices [3], skyrmions [4], etc., became objects of great theoretical and experimental interest. These configurations are direct manifestations of macroscopic coherence of BEC and many of them were repeatedly created and detected.

In our previous work [5] it has been shown that yet another stable object, namely atomic Bose JV, can exist in a long Bose Josephson junction (BJJ) formed by two parallel coupled quasi-1D atomic waveguides. Such circulating atomic supercurrents represent a neutral analog of the Josephson vortex studied in superconducting Josephson junctions in great detail [6]. While bearing some similarities with the charged case, the absence of the Meissner effect makes the local formulation of the BJJ solution possible only in a quasi-1D geometry. The most interesting feature of the Bose JV is its interconversion into a dark soliton (DS) [5]. Accordingly, the description of the Bose JV necessarily involves both the phase and the amplitude of the wavefunction. This instability, which can be controlled by tuning the Josephson coupling, may potentially be utilized in several ways [5]. Here we show that the Berry phase term is responsible for a force produced on the JV by a time-dependent difference of the chemical potentials η applied between the waveguides. Once the JV speed as a whole reaches a certain critical value, the instability destroying the supercurrent circulation develops so that the JV transforms into a moving DS (grey soliton) which is essentially insensitive to η . We also discuss how the phase imprinting method and the interference after some free expansion can be employed for creating and detecting the JV. As it turns out, the relative phase between the waveguides is quite insensitive to the characteristics of the imprinting beams once certain topological requirements are satisfied. The JV introduces a *tangential* feature into the interference pattern.

II. JOSEPHSON VORTEX AND BERRY PHASE EFFECT

A. Phenomenology of the Bose JV

Here we will employ generic phenomenological description of the Bose JV which addresses the Berry phase induced force and the critical speed effect regardless of a particular model of the BJJ. The JV is characterized by spatially localized distributions of persistent currents $J_{1,2}(x)$ along the first and the second waveguides, respectively. The sum $J_+ = J_1 + J_2$ represents the total linear momentum density, which must be zero for the stationary JV. The difference $J_- = J_1 - J_2$ characterizes internal circulation of the supercurrent, which forms spontaneously when the Josephson coupling γ becomes less than some critical value γ_c [5]. The minimal effective Lagrangian can be formulated in terms of the total soliton momentum $P(t) = \int dx J_+(x)$, its center of mass velocity $V(t) = \dot{X}_0$, the circulation of the supercurrent $J(t) = \int dx J_-(x)$ (we consider contributions from the tunneling currents negligible) and the corresponding canonically conjugate variable $Q(t)$. It has a form

$$\mathcal{L}_{eff} = \dot{X}_0 P + \dot{Q} J - \mathcal{H}_{eff}, \quad (1)$$

with the effective Hamiltonian being

$$\mathcal{H} = \frac{P^2}{2M_+} + \frac{Q^2}{2M_-} + \alpha(\gamma - \gamma_c)J^2 + c_1 J^4 - c_2 \eta P J + c_3 J^2 P^2. \quad (2)$$

where M_+ , M_- , $\alpha > 0$, $c_1 > 0$, $c_2, c_3 > 0$ are phenomenological coefficients dependent on a particular form of a microscopic description. These coefficients will be determined later within the variational approach applied to the model [5]. The Lagrangian (1,2) describes the spontaneous formation of the circulation $J \neq 0$ for $\gamma < \gamma_c$ [5] ($c_1 > 0$ insures stability beyond linear approximation) as well as coupling between the center of mass motion and the internal circulation. The term $\sim c_3$ describes the effect of the critical velocity: as $P \sim V$ exceeds some critical value, the effective coefficient $\alpha(\gamma - \gamma_c) + c_3 P^2$

becomes positive, which restores the time-reversal symmetry so that the circulation $J = 0$. This term is symmetric with respect to the exchanging of the waveguides. The term $\sim c_2$ describes the effect of the force induced by the chemical potential difference. Its nature can be understood as follows. When $\eta \neq 0$, a number of atoms $\sim \eta$ starts tunneling between the waveguides in the direction of smaller chemical potential. Accordingly, while one waveguide loses its total linear momentum $\sim \eta J$, the second gains it. Hence, the total momentum P attains a nonzero value $\sim \eta J$.

In the presence of dissipation one should introduce the dissipative function in terms of the velocities \dot{X}_0 and \dot{Q} as

$$\mathcal{F} = \frac{\dot{X}_0^2}{2\sigma_+} + \frac{\dot{Q}^2}{2\sigma_-}, \quad (3)$$

with some kinetic coefficients $\sigma_{\pm} > 0$. Then the standard variational procedure with respect to the conjugate variables yields the equations of motion

$$V - \left(\frac{1}{M_+} + 2c_3 J^2 \right) P - c_2 \eta J = 0, \quad (4)$$

$$\dot{P} + \frac{V}{\sigma_+} = 0, \quad (5)$$

$$\dot{Q} - 2(\alpha(\gamma - \gamma_c) + c_3 P^2) J^2 - 4c_1 J^3 - c_2 \eta P = 0, \quad (6)$$

$$\dot{J} + \frac{Q}{M_-} + \frac{\dot{Q}}{\sigma_-} = 0. \quad (7)$$

Let's, first, consider the case $\eta = 0$ and small J close to the equilibrium. Then, eq.(4) gives $P = M_+ V$. For simplicity, we also consider the case of negligible dissipation with respect to the center of mass motion ($\sigma_+ \rightarrow \infty$), so that P is a conserved quantity as seen from eq.(5). Close to the equilibrium one can set $Q = 0$ in eqs.(6,7) and obtain $-2(\alpha(\gamma - \gamma_c) + c_3 M_+^2 V^2) J^2 - 4c_1 J^3 = 0$. This yields the critical velocity

$$V_c = V_1 \sqrt{\gamma_c - \gamma}, \quad (8)$$

above which only trivial solution $J = 0$ can exist, where $V_1 = \sqrt{\alpha/(c_3 M_+^2)}$.

When $V \ll V_c$, one can ignore the term $\sim c_2$ in eq.(6) and consider $J \neq 0$ as a fixed quantity in eqs.(4,5) for $\eta(t) \neq 0$. Then, excluding P , one finds that the center of mass velocity obeys the equation

$$\dot{V} + \frac{V}{M_+ \sigma_+} = \frac{f(t)}{M_+}, \quad f(t) = c_2 M_+ J \eta, \quad (9)$$

where we have ignored the term $\sim c_3$ in eq.(4). As discussed above, the term $f(t)$ describes the force induced by time dependence of the difference of the chemical potentials η . The relation of this force to the Berry phase term in the full "microscopic" action will be considered below.

B. Variational approach

It is worth noting that all the phenomenological coefficients can be derived from a "microscopic" Lagrangian and a dissipative function. Here we will use a simplified approach which ignores dissipation and will consider model [5] as the "microscopic" Lagrangian. In terms of the fields $\psi_{1,2}$ describing each waveguide the Lagrangian,

$$\mathcal{L} = \mathcal{L}_B - \mathcal{H}, \quad (10)$$

is given by the Berry term

$$\mathcal{L}_B = \text{Re} \int dx \left[i\hbar(\psi_1^* \dot{\psi}_1 + \psi_2^* \dot{\psi}_2) \right], \quad (11)$$

and by the Hamiltonian

$$\mathcal{H} = \mathcal{H}_1 + \mathcal{H}_2 + \mathcal{H}_{12}, \quad (12)$$

consisting of the single waveguide terms

$$\mathcal{H}_k = \int dx \left[\frac{\hbar^2}{2m} |\nabla \psi_k|^2 + \frac{g}{2} |\psi_k|^4 - \mu_k |\psi_k|^2 \right], \quad (13)$$

with $k = 1, 2$, and of the contribution which describes the Josephson tunneling between the waveguides

$$\mathcal{H}_{12} = - \int dx \gamma (\psi_1^* \psi_2 + \psi_2^* \psi_1), \quad (14)$$

where μ_k are waveguide's chemical potentials and the integration $\int dx \dots$ is performed along the waveguides.

The equations of motion following from eqs.(10-14) in the units $\hbar = 1, m = 1$, with the unit of length given by the healing length $l_c = 1/\sqrt{\mu}$ for $\mu = (\mu_1 + \mu_2)/2$ and the unit of time determined by $t_0 = 1/\mu$, are

$$i\dot{\psi}_1 = -\frac{\nabla^2}{2} \psi_1 - (1 + \eta) \psi_1 + |\psi_1|^2 \psi_1 - \nu \psi_2; \quad (15)$$

$$i\dot{\psi}_2 = -\frac{\nabla^2}{2} \psi_2 - (1 - \eta) \psi_2 + |\psi_2|^2 \psi_2 - \nu \psi_1. \quad (16)$$

Here the wave functions were transformed as $\psi_k \rightarrow \sqrt{n_0} \psi_k$, where $n_0 = \mu/g$ is the average 1D density of a single uncoupled ($\gamma = 0$) waveguide; the quantity ν represents the dimensionless Josephson coupling $\nu = \gamma/\mu$, and η stands for the difference of chemical potentials rescaled by 2μ . These equations admit exact JV stationary solution discussed in detail in ref.[5]. For small velocity of the JV, it is natural to use the variational ansatz which coincides with the stationary solution at $V = 0$. Thus, we choose

$$\Psi_{1,2} = \sqrt{n_{1,2}} \text{th}(s(x - X_0(t))) + \frac{i\sqrt{s}Q_{1,2}}{\text{ch}(s(x - X_0(t)))} \quad (17)$$

with the parameter s giving the JV size. The bulk densities $n_{1,2}$ can be obtained in the thermodynamical limit (when no JV is present) from eqs.(15,16). Since we are

interested in small deviations only, the corresponding explicit expressions are

$$n_{1,2} = (1 + \nu) \left(1 \pm \frac{\eta}{1 + 2\nu} + o(\eta^2) \right), \quad (18)$$

where the indexes 1, 2 correspond to \pm , respectively.

The stationary solution [5] can be obtained from the ansatz (17) by setting $X_0 = \text{const}$, $\sqrt{s}Q_1 = -\sqrt{s}Q_2 = \pm\sqrt{1-3\nu}$ and $s = 2\sqrt{\nu}$ (compare with ref.[5]). Considering complex $Q_{1,2}$ and real X_0 as slow dynamical variables, one can substitute the ansatz (17) into the Lagrangian (10-14) and perform explicit integration over x . This procedure generates the effective Lagrangian \mathcal{L}_e in terms of the variables $Q_{1,2}$, X_0 , s and their time-derivatives. Obviously, such procedure is in line with separation of fast and slow variables, so that only slow dynamics should be considered to full extent. Close to the interconversion instability ($\nu \approx \nu_c = \gamma_c/\mu$), the slow variables are X_0 and J . The variable s describes fast adjustment of the JV size. It is important that it is not dynamical within the chosen ansatz. Indeed, as can be seen, the effective Lagrangian does not contain \dot{s} . The choice of s is dictated by conservation of total number of particles during a dynamical evolution of the other parameters. Calculating the depletion δN of the number of particles caused by the presence of the JV, we find

$$\delta N = -\frac{2(n_1 + n_2)}{s} + 2(|Q_1|^2 + |Q_2|^2) = C_N, \quad (19)$$

where the constant C_N is determined for the stationary JV by setting all the time derivatives to zero and minimizing the effective energy with respect to $Q_{1,2}$ and s . Considering small values η , it is enough to set $n_1 + n_2 = 2(1 + \nu)$, which is the equilibrium value. Here we will consider values $Q_{1,2} \rightarrow 0$, so that the explicit solution of eq.(19) for s becomes

$$s = \sqrt{1 + \nu} + \frac{1 - 3\nu}{2\sqrt{1 + \nu}} - \frac{|Q_1|^2 + |Q_2|^2}{2}. \quad (20)$$

As discussed in ref.[5], the value $\nu = \nu_c = 1/3$ is the critical point below which the JV forms spontaneously from the DS. Thus, the smallness of $Q_{1,2}$ automatically implies a proximity to the critical point. Then, for consistency of the effective action expressed in powers of $Q_{1,2}$, the value ν should be set to ν_c except in the quadratic term vanishing at the critical point.

It is worth discussing, first, the structure of the Berry-term part (11) of the full action. As mentioned above, the cross term $\sim \eta P J$ leading to the force on the JV $\sim \dot{\eta}$ in the Lagrangian (1) can be viewed as generated by the Berry phase effect. Indeed, the Berry part is $\mathcal{L}_B = \int dx (-\rho_1 \dot{\varphi}_1 - \rho_2 \dot{\varphi}_2)$, where ρ_k and φ_k are density and the phase, respectively, in the k -th waveguide. In the static solution [5] as well as in the ansatz (17) each phase changes by $\pm\pi$, so that, e.g., if at $x = -\infty$ one finds $\varphi_1 = \varphi_2 = 0$, then, at $x = +\infty$ there is $\varphi_1 - \varphi_2 = 2\pi$. If the JV is moving slowly, then

$\dot{\varphi}_k \approx \dot{X}_0 \nabla \varphi_k$. Thus, a substitution into the Berry part gives $\mathcal{L}_B \approx \dot{X}_0 \int dx (\rho_1 \nabla \varphi_1 + \rho_2 \nabla \varphi_2) \approx \pi \dot{X}_0 (\rho_1 - \rho_2)$, where spatial variations of the densities are ignored. Flipping the time derivative and realizing that $\rho_1 - \rho_2 \sim \eta$, one finds $\mathcal{L}_B \sim -X_0 \dot{\eta}$, which is the work done while making a displacement X_0 by the force $\sim \dot{\eta}$.

The relation between the observables P , J can be obtained as a result of substituting the ansatz (17) into (11). This yields $\mathcal{L}_B = \dot{X}_0 P - 2(\dot{B}_+ Q_+ + \dot{B}_- Q_-)$, where $Q_+ = \text{Re}(Q_1 + Q_2)$, $Q_- = \text{Re}(Q_1 - Q_2)$, $B_+ = \text{Im}(Q_1 + Q_2)$ and $B_- = \text{Im}(Q_1 - Q_2)$. The total momentum $P = -i \int dx (\psi_1^* \nabla \psi_1 + \psi_2^* \nabla \psi_2)$ and the supercurrent circulation $J = -i \int dx (\psi_1^* \nabla \psi_1 - \psi_2^* \nabla \psi_2)$ are given as

$$P = -\pi(1 + \nu)^{3/4} \left[Q_+ + \frac{\eta Q_-}{2(1 + 2\nu)} \right], \quad (21)$$

$$J = -\pi(1 + \nu)^{3/4} \left[Q_- + \frac{\eta Q_+}{2(1 + 2\nu)} \right]. \quad (22)$$

Thus, the parameters Q_{\pm} can uniquely be expressed in terms of P , J . In particular, $Q_+ \sim P$ for $\eta = 0$. The Berry phase effect discussed above is reflected in the part $\sim \eta$ of eq.(21). It is also clear that the variable conjugated to J in eq.(1) is $Q \sim B_-$. Further analysis shows that the quantity $B_+ = \text{Im}(Q_1 + Q_2)$ enters \mathcal{L}_B in a combination $\sim \dot{B}_+ P - r_b B_+^2 + o(B_+^4)$ with some $r_b > 0$. Thus, B_+ would generate higher time derivatives with respect to X_0 , which should be neglected as long as the JV motion is slow. Accordingly, it is reasonable to set $B_+ = 0$ in eq.(17), so that $Q_{1,2}$ are chosen in the form

$$Q_{1,2} = \frac{Q_+ \pm Q_-}{2} \pm i \frac{B_-}{2}, \quad (23)$$

with the indexes 1, 2 corresponding to \pm , respectively. Finally, employing the ansatz (17,23) in the "microscopic" Lagrangian (10-14) and expressing the variables (23) in terms of the observables P , X_0 , Q , J as described above one arrives at the effective Lagrangian in the form (1), where the coefficients (in the chosen units) are

$$\frac{1}{M_+} = -\frac{\sqrt{3}}{2\pi^2}, \quad (24)$$

$$\frac{1}{M_-} = \frac{32\pi^2}{27\sqrt{3}}, \quad (25)$$

$$\alpha(\gamma - \gamma_c) = \frac{3\sqrt{3}}{4\pi^2} \left(\nu - \frac{1}{3} \right), \quad (26)$$

$$c_1 = \frac{3\sqrt{3}}{128\pi^4}, \quad (27)$$

$$c_2 = \frac{2\sqrt{3}}{5\pi^2}, \quad (28)$$

$$c_3 = \frac{9\sqrt{3}}{64\pi^4}. \quad (29)$$

As discussed above, in these expressions the difference $\nu - \nu_c$ has been ignored except in the quadratic coefficient (26), which determines the instability. It is worth noting

that far from the instability $\nu \ll \nu_c$ no simple expansion for the effective Lagrangian in terms of powers of $Q_{1,2}$ can be obtained. Accordingly, the expressions would become much more complicated.

C. Numerical simulation of the Berry phase effect

Sensitivity to the difference of the chemical potentials η can be a useful tool for manipulation of the JV position in the junction. To demonstrate this numerically we used η as an externally controlled variable to displace the JV on a distance much greater than its size and than to return it to its original position. The result of the simulations of the full system (15, 16) is displayed on FIG.1. The plot on the left represents density of a single waveguide by the intensity of white color. The dark curve is a trajectory of the JV center, where its density is minimal. Shown on the right, the time-dependence η is chosen as $\eta(t) = 0.1 \sin(\frac{\pi t}{125})$. The simulations have been performed with the dissipative term introduced in ref.[5].

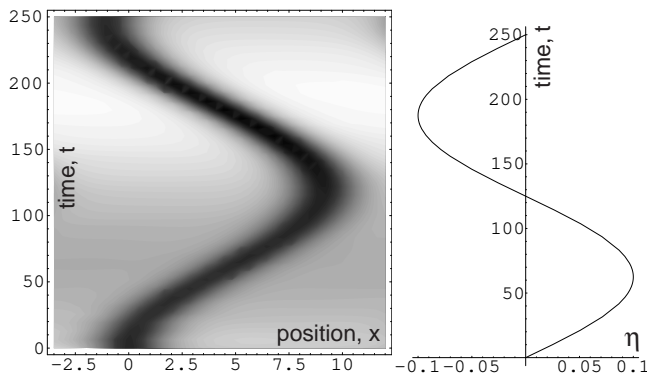


FIG. 1: Motion of the JV along the junction (left) generated by change of relative chemical potential η (right) from numerical simulations of the system (15, 16). Here $\nu = 0.1$, and the dissipative term from ref.[5] is given by the value of the kinetic parameter $\tilde{\sigma} = 2$.

III. CREATION BY PHASE IMPRINTING

The JV can be formed as a result of the decay of the DS, once the Josephson coupling γ is reduced below a critical value γ_c (or, in the chosen units, ν , with the critical value being $\nu_c = 1/3$) [5]. An alternative method is the phase imprinting. It is already a well established experimental tool for creation of the DS [1]. It consists of exposing a BEC to a pulse of a far detuned laser beam which acts as a temporary external potential $U(x, t)$. According to the impulse approximation, the duration of the pulse δt must be short compared to the correlation time of the condensate $t_0 = 1/\mu$, so that no change of the

BEC density occurs during the pulse — atoms just acquire finite speeds without performing any significant displacements. The phase, on the other hand, accumulates

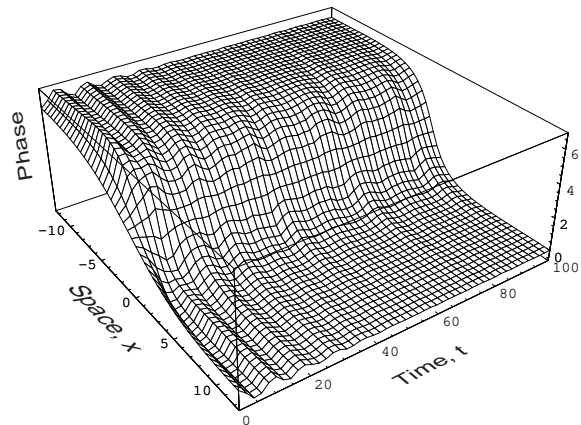


FIG. 2: Evolution of the relative phase after the imprinting as follows from eqs.(15,16). Small dissipative term discussed in ref.[5] with $\tilde{\sigma} = 6$ has been added; $\nu = 0.1$.

according to $\delta\varphi(x) = \int dt U(x, t)$ and the wave function ψ before the pulse is transformed as $\psi \rightarrow e^{-i\delta\varphi}\psi$ after the pulse. To create a DS, one needs to expose a half-plane of an elongated BEC to a laser pulse with a spatial variation reminiscent of the typical DS phase profile (the π -step). In order to produce the JV, one needs to apply a pulse with spatial profiles $U_{1,2}(x, t)$ specific for each waveguide. These should reflect the structure of the JV phases in each waveguide: $\varphi_{1,2} = 0$ at ,e.g., $x = -\infty$ and $\varphi_1 = -\varphi_2 = \pm\pi$ at $x = +\infty$, with smooth transition in between at a typical length comparable to the JV size $= 1/(2\sqrt{\nu})$. Accordingly, $U_{1,2}(x, t) = 0$ at $x = -\infty$ and $U_1(x, t) = -U_2(x, t)$ at $x = +\infty$, with the "crossover" region being approximately equal to the JV size and the time integral $\int dt U_1(x, t) = \pi$ at $x \rightarrow +\infty$.

It is important to note that, once the above "topological" requirements are satisfied, the JV forms with minimal disturbances regardless of other details of the laser beams profiles. The most robust characteristic of the evolving solution turns out to be the phase difference between the waveguides. In the case of the DS, the complete density depletion must form at the DS center. Thus, the adjustment is accompanied by a strong perturbation in the form of the density waves [1]. The depletion at the JV center is also strong, if ν is close to the critical value $1/3$. Accordingly, the densities in each waveguide will experience significant perturbations. Yet, the phase difference relaxes quite smoothly to the equilibrium profile. To demonstrate this feature, we ran the numerical simulations with the initially imprinted profile of the phases given by the tanh-type variations of the light intensities as described above. The result of the following evolution of the phase difference is represented on FIG.2. As can be seen, the equilibrium phase profile establishes after

few relatively small oscillations even though the initial extension of the (imprinted) phase was about two times longer than the equilibrium JV size.

IV. DETECTION BY INTERFERENCE

Experimental visualization is typically done by absorption imaging [7, 8, 9], with its intensity proportional to the density n of the expanding cloud. In contrast to bulk vortices, which can be detected by observing their cores, the JV does not have a core. Yet, the phases exhibit the π -jumps. Thus, the interference of the expanding clouds released from the waveguides should demonstrate a corresponding feature.

In quasi-1D regime a good approximation for the waveguides wave functions in transverse directions is a product of Gaussians $G(y, z) = \exp(-(y^2 + z^2)/2d^2)$. Thus, in 3D, the two waveguides separated by a distance $2z_0$ can be described by the following ansatz:

$$\Psi_0(\vec{R}) = \Psi_0^+ + \Psi_0^- \quad (30)$$

$$\Psi_0^\pm = f(x)\psi_{1,2}(x)G(y, z \pm z_0) \quad (31)$$

where $\psi_{1,2}(x)$ are the solutions (17) corresponding to either the DS ($Q_{1,2} = 0$) or the JV and the sign \pm is different for different waveguides. The envelope $f(x) = (1 - (4x^2/L))$, with L , the axial system size, being much larger than the JV, reflects finiteness of the BEC clouds.

As long as the transverse dimension d is much smaller than any axial feature, the expansion occurs primarily in the transverse direction. Thus, the density decreases, practically instantaneously, so that the expansion is essentially free of interaction. This can be formulated as the requirement $(d/l_c)^2 \ll 1$. Indeed, the mean-field interaction is given by the chemical potential $\mu \sim n(t)$, where $n(t) \sim 1/R^2(t)$ stands for a typical density of the expanding cloud scaled by its radius $R(t) \approx \sqrt{d^2 + (t/d)^2}$ (in chosen units). The interaction-induced additional phase shift can be estimated as $\Delta\phi \approx \int_0^\infty \mu dt \sim \int_0^\infty n dt \approx (d/l_c)^2 \ll 1$, where the initial density is taken as $n = 1$ in the chosen units. Hence, under this condition, the density after time t of free expansion becomes

$$n(\vec{R}, t) = \frac{1}{t^3} \left| \int d^3 R' \exp\left(\frac{i(\vec{R} - \vec{R}')^2}{2t}\right) \Psi_0(\vec{R}') \right|^2. \quad (32)$$

A numerical factor in (32) is set to 1, because it defines only overall intensity (not the structure) of the absorption image.

When two expanding uniform BECs overlap they form an interference pattern (IP) of parallel fringes [7, 8]. The specific signature of a rotational vortex in the IP is a so-called edge dislocation. It was predicted in ref.[10] and then seen experimentally in ref.[9]. Here we will discuss how the JV can be recognized in the IP.

For any feature with a size $\sim L_s$ comparable with the healing length to become optically resolvable it must be

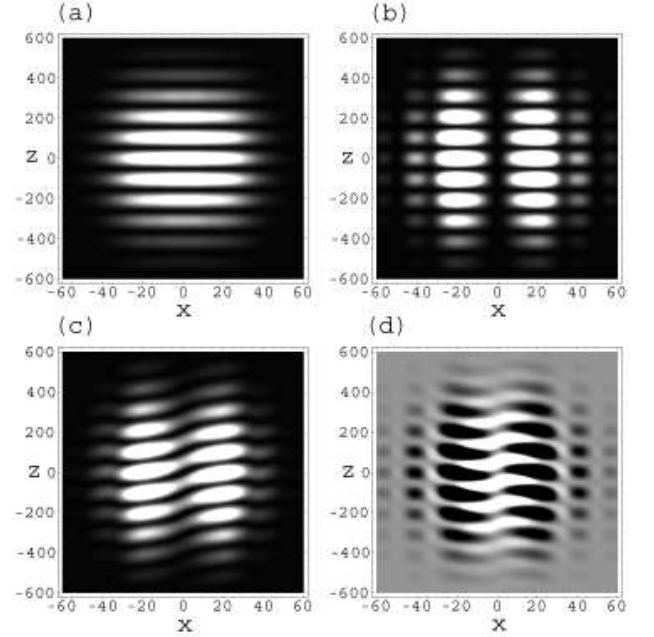


FIG. 3: Interference patterns of two expanded overlapping BEC clouds released from the waveguides as given by direct numerical integration of (32). Waveguides initially contained: (a) uniform BECs, (b) two DS aligned at $x = 0$, (c) JV solution located at $x = 0$. The image (d) is the relative intensity between (b) and (c); $\nu = 0.01$, $t = 100$, $d = 2^{-3/2}$, $z_0 = 3$.

enlarged (typically about 10 times) during the expansion. We consider the situation when axial expansion of the cloud of length L can be ignored. This imposes the limitation $\sqrt{t} \ll L$ in the chosen units. We also ignore quasi-1D thermal fluctuations. In other words, the phase-correlation length L_φ [11] is taken larger than the system size L . In reality this is too strong of a requirement — the discussed feature can be seen when $L_\varphi \geq L_s$.

Employing the ansatz (30,31), the density after time t (such that $R(t) \gg d$, that is, $t \gg d^2$) becomes

$$n(x, y, z) = \frac{e^{-\frac{(y^2+z^2)d^2}{t^2}}}{t^3} \left| \int dx_1 e^{-ix_1^2/2t} f(x_1) \left(\sin\left(\frac{zz_0}{t}\right) \cos\left(\frac{xx_1}{t}\right) \psi''(x_1) + i \cos\left(\frac{zz_0}{t}\right) \sin\left(\frac{xx_1}{t}\right) \psi'(x_1) \right) \right|^2 \quad (33)$$

where the overall factor is dropped, and $\psi'(x) = \sqrt{1 + \nu} \tanh(sx)$ and $\psi''(x) = Q_0 / \cosh(sx)$ are, respectively, the real and imaginary parts of the JV solution [5] given by $s = 2\sqrt{\nu}$, $Q_0 = \sqrt{1 - 3\nu}$. It is instructive to consider three distinctive cases: i) two uniform condensates, which can be reproduced from eq.(33) by setting $\psi' = 0$ and $\psi'' = 1$; ii) two identical DSs at $x = 0$, which can be obtained by setting $\psi'' = 0$; and iii) the JV. In the case i), taking the limit $L \rightarrow \infty$ and performing explicit integration, one finds the well known parallel

fringes $n(x, y, z) \sim \cos^2(zz_0/t)$. In the case ii), there is a zero at $x = 0$. Its width can be estimated from eq.(33) as $\delta x \approx \sqrt{t}$ in the limit $\sqrt{t} \gg 1/s$, that is, when the DS length $L_s = 1/s$ has expanded significantly: $L_s \ll t/L_s$. The actual density profile can be obtained analytically for $1/s \ll |x| \leq \sqrt{t}$ as

$$n_{DS}(x, y, z) = \frac{4(1+\nu)e^{-\frac{(y^2+z^2)d^2}{t^2}}}{t^3} x^2 \cos^2\left(\frac{zz_0}{t}\right). \quad (34)$$

It features the parallel fringes with the central zero as shown in Fig.3b.

The JV IP can easily be understood by analyzing the vicinity $x = 0$. Indeed, for $1/s \ll |x| \leq \sqrt{t}$, the $\tanh(sx)$ function can be replaced by a step function and $Q_0/\cosh(sx)$ effectively becomes $\delta(x) \int dx Q_0/\cosh(sx) = \pi Q_0 \delta(x)/s$. Thus, the density profile due to the JV becomes

$$n_{JV}(x, y, z) = \frac{e^{-\frac{(y^2+z^2)d^2}{t^2}}}{t^3} (2\sqrt{1+\nu} \cos(\frac{zz_0}{t}) x + \frac{\pi\sqrt{1-3\nu}}{2\sqrt{\nu}} \sin(\frac{zz_0}{t}))^2. \quad (35)$$

The profile of the zeros of the density $n = n(x, z, t)$ defines the feature specific for the JV. In the DS case, zeros belong to the set of mutually orthogonal lines $x = 0$ and $z = \pi(n + 1/2)t/z_0$, with n integer. In the JV case, represented by eq.(35), the lines of zeros do not cross any more and obey the condition

$$x = \frac{\pi}{4} \sqrt{\frac{1-3\nu}{\nu(1+\nu)}} \tan\left(\frac{sz}{t}\right) \quad (36)$$

The inclined tangential feature seen on Fig.3c is a consequence of the smooth relative phase change from 0 to 2π in the JV. Direct numerical integration of (32) with initial condition (30,31) confirms this result. On Fig.(3) we have plotted the column density (integrated over y) at $t = 100$ ($t = 50ms$ in usual units, which is a typical

experimental expansion time after which the absorption image is taken).

It should be noted that the above presented IP corresponds to the case when the separation between the waveguides z_0 is significantly larger than the transverse extension d . Obviously, in this situation the tunneling ν is essentially zero. If one tries to decrease z_0/d , the visibility of the fringes worsens due to the exponential factor in (33) so that for $z_0/d \sim 1$ just one central fringe is seen. Thus, in order to achieve a good resolution, the clouds should be quickly separated from each other and, then, immediately released. Under these conditions, the JV solution formed at a closed proximity between the waveguides will have no time to be distorted by the inter-particle interactions after the tunneling is cut off. Obviously, the duration of the waveguides' separation from some distance $z_0 \approx d$ (when the tunneling is finite) to $z_0 \approx 10d$ (when the tunneling is, practically, zero) is limited from below by the inverse frequency $\approx d^2$ of the radial confinement. From above, it is limited by the axial response time $1/\mu \approx l_c^2$. This requirement can safely be satisfied if $(d/l_c)^2 \ll 1$, that is, in the quasi-1D regime.

V. CONCLUSION

The atomic Bose Josephson vortex can be created by the phase imprinting technique and detected due to its particular feature in the column density by absorption imaging performed after some ballistic expansion. The Josephson vortex can be controllably displaced by creating disbalance of chemical potentials between the waveguides. This effect could be found useful in future experiments.

VI. ACKNOWLEDGEMENT

This work is supported by the NSF grant PHY-0426814 and by the PSC-CUNY grant 66556-0035.

-
- [1] S. Burger, K. Bongs, S. Dettmer, W. Ertmer, K. Sengstock, A. Sanpera, G. V. Shlyapnikov, M. Lewenstein, Phys. Rev. Lett. **83**, 5198 (1999); B.P. Anderson, P.C. Haljan, C.A. Regal, D.L. Feder, L.A. Collins, C. W. Clark, E. A. Cornell, *ibid.* **86**, 2926 (2001); J. Denschlag, J. Denschlag, J. E. Simsarian, D. L. Feder, C. W. Clark, L. A. Collins, J. Cubizolles, L. Deng, E. W. Hagley, K. Helmerson, W. P. Reinhardt, S. L. Rolston, B. I. Schneider, W. D. Phillips, Science **287**, 97 (2000).
 - [2] Kevin E. Strecker, Guthrie B. Partridge, Andrew G. Truscott and Randall G. Hulet, Nature (London) **417**, 150 (2002); L. Khaykovich, F. Schreck, G. Ferrari, T. Bourdel, J. Cubizolles, L. D. Carr, Y. Castin, C. Salomon, Science **296**, 1290 (2002).
 - [3] A. Fetter and A. Svidzinsky, J. Phys.: Condens. Matter **13**, R135 (2001).
 - [4] C. M. Savage and J. Ruostekoski, Phys. Rev. Lett. **91**, 010403 (2003).
 - [5] V. M. Kaurov and A. B. Kuklov, Phys. Rev. A **71**, 011601(R) (2005).
 - [6] A. Barone, G. Paterno, *Physics and Applications of the Josephson Effect*, John Wiley & Sons, New York - Singapore, 1982.
 - [7] M.R. Andrews, C.G. Townsend, H.-J. Miesner, D.S. Durfee, D.M. Kurn, and W. Ketterle, Science **275**, 637-641 (1997).
 - [8] Y. Shin, M. Saba, T.A. Pasquini, W. Ketterle, D.E. Pritchard, A.E. Leanhardt, Phys. Rev. Lett. **92**, 050405 (2004).
 - [9] S. Inouye, S. Gupta, T. Rosenband, A. P. Chikkatur,

- A. Gorlitz, T. L. Gustavson, A. E. Leanhardt, D. E. Pritchard, and W. Ketterle, Phys. Rev. Lett. **87**, 080402 (2001); F. Chevy, K. W. Madison, V. Bretin, and J. Dalibard, Phys. Rev. A **64**, 031601(R) (2001);
- [10] Eric L. Bolda and Dan F. Walls, Phys. Rev. Lett. **81**, 5477 (1998); J. Tempere and J. T. Devreese, Solid State Commun. **108**, 993 (1998).
- [11] D.S. Petrov, G.V. Shlyapnikov, and J.T.M. Walraven, Phys. Rev. Lett. **85**, 3745 (2000); *ibid.* **87**, 050404 (2001); S. Dettmer, D. Hellweg, P. Ryytty, J. J. Arlt, W. Ertmer, K. Sengstock, D. S. Petrov, G. V. Shlyapnikov, H. Kreutzmann, L. Santos, M. Lewenstein, *ibid.* **87**, 160406 (2001).